

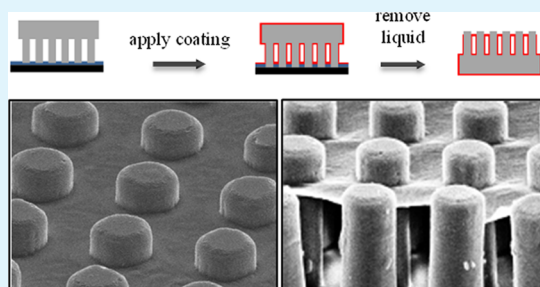
Fabricating Polymer Canopies onto Structured Surfaces Using Liquid Scaffolds

Benny Chen, Robert J. Frank-Finney, and Malancha Gupta*

Mork Family Department of Chemical Engineering and Materials Science, University of Southern California, Los Angeles, California 90089, United States

ABSTRACT: In this work, we study the use of initiated chemical vapor deposition in conjunction with liquid scaffolds to deposit polymer canopies onto structured surfaces. Liquid is applied to micropillar and microstructure surfaces to act as a scaffolding template such that the deposited polymer films take the shape of the liquid surface. Two methods for directing the location of the scaffolding liquid were examined. In the first method, high surface tension liquids rest in a Cassie–Baxter state over the structured surfaces, allowing for control over the canopy location and size by varying the position and volume of the liquid. In the second method, the structured surfaces are inverted onto a thin layer of low surface tension liquid, allowing the coverage and height of the canopy to be controlled by varying the area and thickness of the liquid layer. Although the canopies demonstrated in this study were fabricated using initiated chemical vapor deposition, the generality of our scaffolding method can easily be translated to other vapor deposition processes.

KEYWORDS: polymers, coatings, chemical vapor deposition, thin films



INTRODUCTION

Modifying surfaces with polymers can provide desirable functionalities such as antimicrobial properties,¹ biocompatibility,² and environmental responsiveness.³ Applying polymers to the surfaces of complex geometries such as trenches and pores can allow the effects of the functionality to be enhanced by the greater surface to volume ratio. For example, electrospun fiber mats can be coated with polymer to make superhydrophobic surfaces,⁴ microtrenches can be modified to immobilize nanoparticles,⁵ and porous media can be coated to facilitate the separation of analytes⁶ and to control drug delivery.⁷

Chemical vapor deposition is an attractive option for forming coatings on complex geometries due to numerous advantages derived from its solventless nature. In contrast, typical solution-based coating processes such as spin coating and spray coating are subject to surface tension effects,⁸ ultimately limiting their application on complex geometries. Many chemical vapor deposition techniques have been used to produce functional polymer coatings such as plasma enhanced chemical vapor deposition⁹ and oxidative chemical vapor deposition.¹⁰ One specific technique that has seen recent advancement is initiated chemical vapor deposition (iCVD). The iCVD technique is a solventless vacuum process that forms polymer coatings directly onto substrates. In this process, monomer and initiator molecules are flown into a reactor chamber where the initiator comes into contact with a heated filament array, which decomposes the initiator into radicals. These radicals can then adsorb onto the surface of the substrate and react with adsorbed monomer to initiate free radical polymerization. The

iCVD process has been used to produce functional coatings that lead to the biocompatibility of medical implants¹¹ and facilitate the separation of molecules.^{12,13} Additionally, the iCVD process can be used to apply conformal coatings onto complex geometries such as porous media,^{12–14} micropillar arrays,¹⁵ and forests of carbon nanotubes with diameters on the order of hundreds of nanometers.¹⁶ The iCVD process has also recently been used to deposit polymers onto low vapor pressure liquids such as ionic liquids and silicone oils to expand the structural control of polymer deposition to include free-standing films,¹⁷ gels,¹⁸ particles,¹⁹ gradient films,²⁰ and microstructured films.²¹

In this study, we explore a liquid scaffolding technique that is used in conjunction with the iCVD process to fabricate polymer canopies onto complex geometries. We demonstrate the capabilities of this technique by directly depositing a variety of polymer canopies over micropillar and microstructure arrays. Unlike previous demonstrations of using liquids with the iCVD process, the liquid scaffolding technique focuses on using the liquid as a template which simultaneously masks the surface while providing structural support for the deposited polymer. After the polymer film is deposited, the liquid is removed to reveal regions that were masked in the process as well as a polymer film that retains the shape of the liquid surface. We explore two methods, the Droplet Method and the Inverted Method, for manipulating the scaffolding liquids such that a

Received: July 19, 2015

Accepted: September 9, 2015

Published: September 17, 2015

variety of polymer canopies can be made using a range of liquids. Unlike physically placing a polymer film on top of the substrate, our fabrication methods directly form canopies on the surfaces allowing for better mechanical stability. Additionally, the Inverted Method has the added capability of controlling the height of the canopy relative to the substrate features. The formation of polymer layers over complex geometries is of interest in fields such as drug release, where the polymer can act as a tunable gatekeeper.^{22–24} Additionally, liquid scaffolding can potentially be applied to other geometries such as microfluidic channels, allowing for the fabrication of polymer membranes within the channels to extend their utility. For example, polycarbonate membranes used within microfluidic channels can prevent the cross-contamination between two regions while allowing for the delivery of reactants across the membrane.²⁵ Although we only demonstrate a few examples of liquid manipulation for generating scaffolding templates, there are many additional strategies that can be employed to control liquids on complex geometries, including the controlled formation of microdrops on top of microposts,²⁶ the controlled infiltration of liquid within textured surfaces,^{27,28} and the capillary rise of liquids between various pillar geometries.^{29,30} Additionally, the methods presented are not limited to iCVD systems since the generality of the strategy can be easily translated to other vapor deposition techniques.

RESULTS AND DISCUSSION

Our group has previously demonstrated the ability to deposit polymers onto low vapor pressure liquids using the iCVD process.^{31,17–21} The surface interactions between the liquid and the polymer determines the initial morphology of the deposited polymer. The surface interaction can be quantified using the spreading coefficient (S):

$$S = \gamma_{LV} * (1 + \cos \theta) - 2\gamma_{PV}$$

where γ_{LV} is the liquid–vapor surface tension, θ is the advancing contact angle of the liquid on the polymer, and γ_{PV} is the polymer–vapor surface tension.³² When the spreading coefficient is positive, it is energetically favorable for the polymer to spread over the surface resulting in thermodynamically stable films, whereas a negative spreading coefficient represents systems where it is favorable for the polymer to reduce contact with the liquid surface resulting in particles. Additional work has demonstrated that it is possible to deposit polymer films on liquids when the system spreading coefficient is negative by using a cross-linker.²¹

We were able to control the fabrication of polymer canopies on top of micropillar arrays by exploiting systems with positive spreading coefficients or by using cross-linkers with systems that have negative spreading coefficients. The fabrication was performed by applying liquid onto the micropillar arrays and then depositing a polymer film using the iCVD process. The liquid acts as a scaffold, serving as a temporary supporting template for the polymer to deposit onto so that upon its removal, the polymer retains the shape of the liquid surface. We focused on two methods for directing liquids on the pillars, each having its own inherent advantages that allow for the fabrication of canopies using liquids with either high or low surface tensions. The Droplet Method (Figure 1a) exploits liquids that rest in the Cassie–Baxter state on top of the pillars, allowing the iCVD process to deposit a polymer film underneath the droplet. This method typically requires liquids

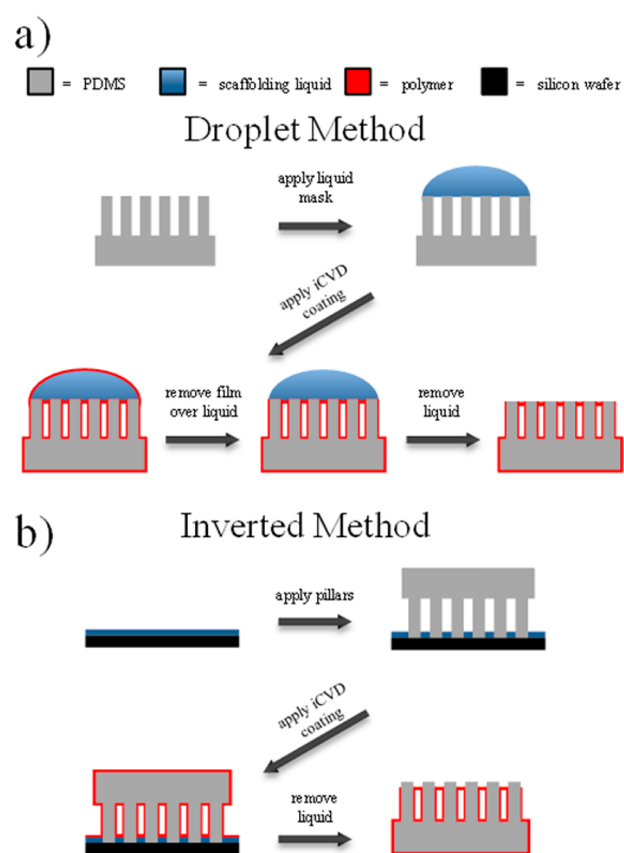


Figure 1. Schematics showing the fabrication of polymer canopies via (a) the Droplet Method and (b) the Inverted Method.

with high surface tensions to generate the Cassie–Baxter state, where the size of the canopy is dictated by the volume of the liquid and the position of the canopy is dictated by the location of the droplet. The Inverted Method (Figure 1b) utilizes the inversion of pillars onto a thin layer of low surface tension liquid such that the iCVD process deposits a polymer film in the spaces between the pillars on top of the liquid. The height of the canopy can be easily controlled using the Inverted Method by altering the thickness of the liquid. Due to the ease of generating thin layers of liquids over large areas, this technique is preferred for fabricating canopies over larger areas.

When using the Droplet Method, it is critical to select systems that allow the liquid to maintain a Cassie–Baxter state, otherwise the liquid will penetrate between the pillars, compromising the ability of the liquid to act as the desired template for canopy fabrication. Many studies have documented the requirements for maintaining a Cassie–Baxter state, where factors such as surface energy and surface roughness have a major influence on droplet stability.^{33–36} Taking these factors into consideration, we chose 1-ethyl-3-methylimidazolium tetrafluoroborate ([emim][BF₄]) as our scaffolding liquid because its high surface tension (55.6 mN/m)³² allows it to easily exist in the Cassie–Baxter state on our PDMS pillar array (height = 60 μm , diameter = 22 μm , and pitch = 18 μm). Canopies were fabricated by applying a droplet onto a pillar array followed by the deposition of a poly-(1*H*,1*H*,2*H*,2*H*-perfluorodecyl acrylate-*co*-ethylene glycol diacrylate) (P(PFDA-*co*-EGDA)) copolymer coating ($S = 18 \text{ mN/m}$), resulting in the formation of a polymer film over the exposed liquid and solid surfaces. Ethylene glycol diacrylate

(EGDA) was used to cross-link the polymer film to increase mechanical strength. The thickness of the coating was $1\ \mu\text{m}$ as measured on a reference silicon wafer. The film residing on top of the droplet was then peeled off with a pair of tweezers such that a subsequent solvent wash removed the $[\text{emim}][\text{BF}_4]$, leaving behind a P(PFDA-co-EGDA) canopy on top of the pillar array. An example of a polymer canopy generated with a $5\ \mu\text{L}$ droplet is depicted in Figure 2. SEM micrographs reveal that

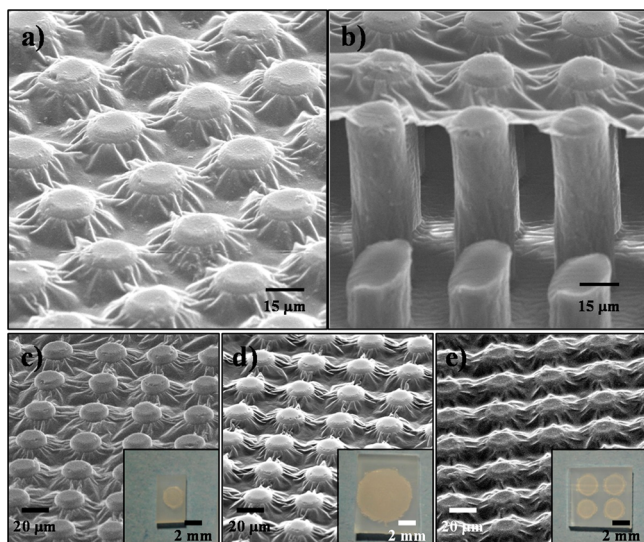


Figure 2. (a) Top down and (b) cross-sectional SEM micrographs of P(PFDA-co-EGDA) canopies fabricated using $[\text{emim}][\text{BF}_4]$ with the Droplet Method. SEM micrographs showing canopies made with (c) a $5\ \mu\text{L}$ droplet, (d) a $100\ \mu\text{L}$ droplet, and (e) $10\ \mu\text{L}$ droplets in a 2×2 array. Optical microscopy images depicting each canopy are provided as an inset in each image.

the canopy forms at the upper rim of the pillars (Figure 2a), leaving the tops of the pillars as native PDMS. A cross-sectional SEM micrograph (Figure 2b) of the sample after it had been cut with a razorblade confirms that the polymer forms a canopy structure over the pillar arrays where the shorter pillars in the front of the image are pillars with their tops severed during the cutting process. A range of droplet sizes from 5 to $100\ \mu\text{L}$ were used to fabricate canopies of varying areas, where larger liquid volumes yielded canopies with larger radii. Using $[\text{emim}][\text{BF}_4]$ droplet volumes of 5 , 10 , and $100\ \mu\text{L}$, we were able to fabricate canopies of approximately 2 , 3 , and $6\ \text{mm}$ in diameter, respectively. Droplet volumes much larger than $100\ \mu\text{L}$ were difficult to use due to the tendency of the droplet to roll off the surface of the pillar array. The resultant canopies are depicted in Figure 2c–e, where the insets show optical microscopy images of the canopies. Figure 2e also demonstrates the ability to selectively place the liquid droplets to pattern the location of the canopies. In this case, we deposited the $10\ \mu\text{L}$ droplets of $[\text{emim}][\text{BF}_4]$ in a 2×2 array before depositing a P(PFDA-co-EGDA) coating. After removing the liquid, the resultant canopies remained at the locations once occupied by the droplets.

The SEM images in Figure 2 show that the canopies are wrinkled. We hypothesize that the wrinkled texture of the canopies is due to anisotropic swelling, which has been shown to be responsible for the wrinkling of other films that are anchored to a solid.³⁷ Our previous studies of iCVD polymerization onto liquids have shown that there is only

surface polymerization in the cases where the monomer is insoluble in the liquid, whereas there is both surface and bulk polymerization in the cases where the monomer is soluble in the liquid.³¹ Since $1H,1H,2H,2H$ -perfluorodecyl acrylate (PFDA) is insoluble in $[\text{emim}][\text{BF}_4]$, whereas ethylene glycol diacrylate (EGDA) is soluble in $[\text{emim}][\text{BF}_4]$, deposition of P(PFDA-co-EGDA) on $[\text{emim}][\text{BF}_4]$ by iCVD results in the formation of heterogeneous layered films, which was confirmed in our previous work.³⁸ During the deposition of polymer, EGDA is able to absorb into the $[\text{emim}][\text{BF}_4]$ and polymerize so that the resultant heterogeneous polymer film is composed of a layer of P(PFDA-co-EGDA) and a layer of polymerized EGDA containing integrated $[\text{emim}][\text{BF}_4]$. After the washing step, the removal of $[\text{emim}][\text{BF}_4]$ likely leads to a volume change within the polymer matrix resulting in the wrinkling of the canopy.

Energy dispersive spectroscopy (EDS) was used to characterize the compositions of the canopy and the tops of the pillars. A scan of the canopy region showed an elemental composition of 66.6% C, 11.1% O, 17.8% F, and 4.5% Si. The high fluorine content is attributed to the poly($1H,1H,2H,2H$ -perfluorodecyl acrylate) (PPFDA) within the P(PFDA-co-EGDA) canopy, while the silicon is attributed to the PDMS from the underlying substrate due to the sampling depth of the analysis method which can exceed $1\ \mu\text{m}$. In contrast, a scan of the top of the pillars showed an elemental composition of 52.4% C, 18.1% O, 4.8% F, and 24.7% Si which is similar to the expected elemental composition of PDMS (50% C, 25% O, 25% Si). The low fluorine content and the relative decrease in oxygen content relative to PDMS suggest that the canopy material exists in small quantities on the top of the pillars. Since we have previously shown that PFDA does not polymerize within the bulk of $[\text{emim}][\text{BF}_4]$ due to insolubility,³¹ the fluorine content is attributed to polymer which was displaced onto the pillar surface during the washing step.

Fabricating canopies using the Droplet Method requires the liquid scaffold to be in a Cassie–Baxter state, limiting the selection of liquids to those with high surface tensions. High surface tension liquids can make it difficult to fabricate canopies over large areas since larger droplet volumes tend to roll off the surface. Furthermore, the Cassie–Baxter state limits control over the height of the canopy since the liquid is required to rest on top of the pillars. In order to expand the viable liquids that can be used to generate canopies and introduce a method of control over the canopy height, we explored an alternative strategy for manipulating the scaffolding liquid. In this second method (Inverted Method), the pillars are inverted onto a thin layer of liquid that was spin coated onto a silicon wafer before applying the iCVD process (Figure 1b). A solvent wash was then used to remove any remaining liquid, revealing a polymer canopy. In contrast to the Droplet Method, the liquids used in the Inverted Method have low surface tensions, allowing them to be easily spin coated into thin layers. For this reason, we chose silicone oil as our model liquid for the Inverted Method. However, since silicone oil is chemically similar to our PDMS pillar material, we precoated the pillars with $100\ \text{nm}$ of PPFDA to prevent any liquid from diffusing into and swelling the pillars. PPFDA was selected because it has previously been shown to act as an effective barrier coating against organic liquids.^{39,13} Using precoated pillars with the Inverted Method, we successfully fabricated P(PFDA-co-EGDA) ($S = 13\ \text{mN/m}$) canopies with a range of heights by spin coating liquid layers of varying thicknesses. The thickness of the coating was $1\ \mu\text{m}$ as

measured on a reference silicon wafer. SEM micrographs of the resultant canopies are shown in Figure 3 with heights of 58 μm

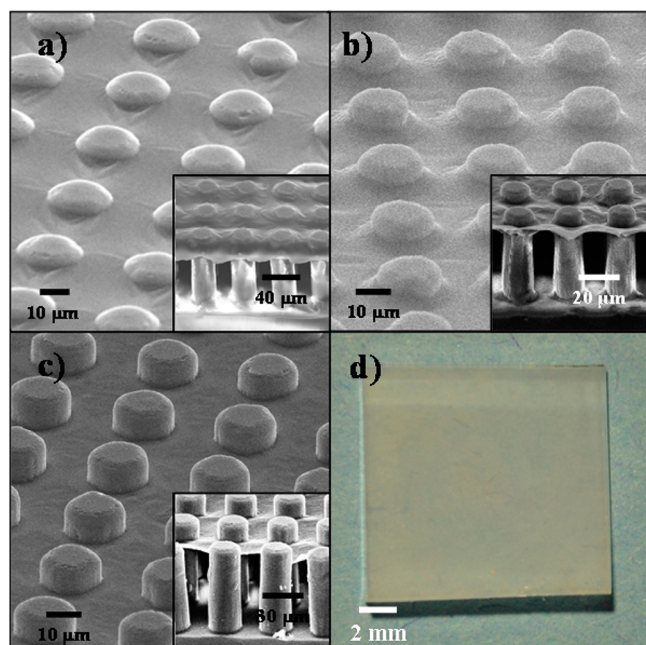


Figure 3. SEM micrographs of P(PFDA-*co*-EGDA) canopies with a height of (a) 58 μm , (b) 50 μm , (c) and 46 μm fabricated using silicone oil with the Inverted Method, where cross-sectional depictions are shown as insets. (d) An optical microscopy image of the 58 μm canopy is also provided, demonstrating the large area of the canopy.

(Figure 3a), 50 μm (Figure 3b), and 46 μm (Figure 3c) with cross-sectional views confirming the canopy structure of the film. In comparison to the Droplet Method canopies, the relative smoothness of the Inverted Method canopies is attributed to the insolubility of either monomer within the silicon oil, preventing the effects of anisotropic swelling. An example of an optical microscopy image of the canopy with a height of 58 μm is depicted in Figure 3d, demonstrating the ability to fabricate canopies over large areas. Although the depicted canopy has an approximate area of a square centimeter, the method can easily be used to make larger canopies by increasing the size of the pillar array and the area of the liquid layer.

EDS analysis was performed on the canopy and the tops of the pillars. A scan of the canopy region showed a composition of 64.1% C, 12.8% O, 18.8% F, and 4.3% Si, which is consistent with the Droplet Method canopy, where the high fluorine content is attributed to the PPFDA within the P(PFDA-*co*-EGDA) canopy and the silicon content is attributed to the underlying PDMS substrate. A scan of the tops of the pillars showed a composition of 56.5% C, 10.7% O, 7.3% F, and 25.5% Si. As expected, there is a significant increase of silicon content which suggests that the canopy does not form on top of the pillar. The relative decrease in oxygen content and increase in carbon and fluorine compared to native PDMS can be explained by the 100 nm precoating of PPFDA which was deposited onto the pillars prior to applying the Inverted Method.

We have demonstrated thus far that canopies can be fabricated using systems with positive spreading coefficients. However, it may be desirable to fabricate canopies comprised of

polymers that yield negative spreading coefficients. Attempts at fabricating canopies using systems with negative spreading coefficients, such as poly(2-hydroxyethyl methacrylate) on [emim][BF₄] or silicone oil, were unsuccessful since the polymer formed particles instead of a film at the liquid surface. However, we were able to successfully fabricate canopies by adding a cross-linker to these systems since the cross-linker can covalently attach growing polymer chains as they deposit on the liquid surface, leading to the formation of a film over the liquid surface.²¹ Using EGDA as a cross-linking agent, we successfully fabricated poly(2-hydroxyethyl methacrylate-*co*-ethylene glycol diacrylate) (P(HEMA-*co*-EGDA)) canopies using both the Droplet Method ($S = -22$ mN/m) and the Inverted Method ($S = -68$ mN/m). SEM micrographs of the resultant P(HEMA-*co*-EGDA) canopies with cross-sectional insets are shown in Figure 4, parts a and b, respectively, where the height of the Inverted Method canopy is 50 μm tall.

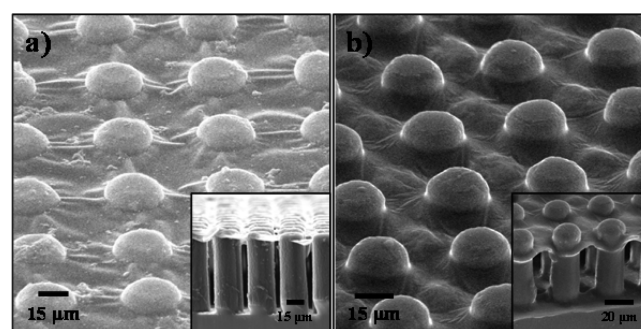


Figure 4. SEM micrographs of P(HEMA-*co*-EGDA) canopies fabricated using (a) the Droplet Method and (b) the Inverted Method, where insets show a cross-sectional view of each sample.

Micropillar arrays function well as a model substrate for demonstrating the Droplet Method and the Inverted Method, but either technique can easily be extended to other geometries. In order to show this concept, we applied both methods on an alternative geometry by converting the pillars into hierarchal microstructures (Figure 5a) using a technique we have

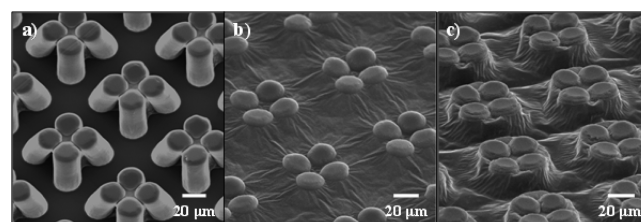


Figure 5. SEM micrographs of (a) PDMS microstructures stabilized with PMMA, and P(PFDA-*co*-EGDA) canopies over microstructures fabricated using (b) the Droplet Method and (c) the Inverted Method.

previously developed.⁴⁰ In this technique, we cast a solution of poly(methyl methacrylate) in acetone onto the pillar surface. Capillary forces produced from solvent evaporation bring the pillars into contact forming microstructures which are then stabilized by poly(methyl methacrylate) welds that form at the interface between the pillars. The successful fabrication of P(PFDA-*co*-EGDA) polymer canopies on these microstructures using the Droplet Method and the Inverted Method are shown in Figure 5, parts b and c, respectively, where the height of the Inverted Method canopy is 46 μm tall.

CONCLUSIONS

We have demonstrated a novel scaffolding technique where low vapor pressure liquids are used in conjunction with the iCVD process to simultaneously act as a mask and temporary supporting template which allows for the fabrication of polymer canopies over micropillar arrays. Two strategies for applying the liquid scaffolds were investigated: (1) the Droplet Method, which uses high surface tension liquids, was used to tune the size of the canopies by selectively controlling the volume of the liquid droplet, and (2) the Inverted Method, which was used to fabricate canopies with a range of heights over large areas using thin layers of low surface tension liquids with varying thicknesses. Systems with negative spreading coefficients that would generally not yield successful fabrication of canopies were overcome through the utilization of a cross-linker, demonstrating that a range of polymer canopies can be synthesized using either method. The generality of each method was also shown by fabricating canopies over an alternative microstructure geometry. Additionally, the methods shown are not restricted to iCVD and can be translated to other vapor deposition systems.

EXPERIMENTAL SECTION

[emim][BF₄] (97%, Sigma-Aldrich), PFDA (97%, SynQuest), di-*tert*-butyl peroxide (98%, Sigma-Aldrich), EGDA (97%, Monomer-Polymer), silicone oil (1000 cSt, Sigma-Aldrich), 2-hydroxyethyl methacrylate (98%, Sigma-Aldrich), trichloro(1*H*,1*H*,2*H*,2*H*-perfluorooctyl) silane (97%, Sigma-Aldrich), glycerol (EMD Chemicals), diiodomethane (99%, Sigma-Aldrich), methanol (Macron, absolute), hexane (98%, Sigma-Aldrich), and poly(methyl methacrylate) (500 000 MW, Varian GPC standards) were used as received without further purification.

Micropillar arrays were fabricated by pouring Sylgard 184 mixed at a base to cross-linker weight ratio of 10:1 into a master mold before curing the mixture at 65 °C for 24 h. The mold was fabricated using standard photolithography by spin coating SU-8 2050 photoresist (MicroChem) before exposing it to UV light through an emulsion transparency mask (CAD/Art Services, Inc.). Prior to molding PDMS pillars, the mold was treated with trichloro(1*H*,1*H*,2*H*,2*H*-perfluorooctyl) silane in a desiccator to reduce the adhesion of cured PDMS, ensuring the easy release of the micropillar arrays. PDMS microstructures were self-assembled by pipetting 10 μL of a 0.5% w/w solution of poly(methyl methacrylate) in acetone onto 0.7 × 0.7 cm² PDMS pillar arrays and allowing the solvent to evaporate overnight prior to use.

All polymer depositions were performed within a custom iCVD reactor chamber (GVD Corp, 250 mm diameter, 48 mm height) equipped with a nichrome filament array (80% Ni, 20% Cr, Omega Engineering) maintained at 240 °C. Di-*tert*-butyl peroxide initiator molecules were flown in at room temperature through a mass flow controller at a rate of 1.0 sccm. All monomer inlet lines were heated to temperatures 20 °C greater than the monomer temperatures to prevent condensation within the lines. P(PFDA-*co*-EGDA) films were synthesized by maintaining a pressure of 70 mTorr and a stage temperature of 30 °C while heating the PFDA and EGDA monomers to a temperature of 50 °C to achieve flow rates of 0.3 and 1.2 sccm, respectively. P(HEMA-*co*-EGDA) films were synthesized by maintaining a pressure of 50 mTorr and stage temperature of 25 °C while heating the 2-hydroxyethyl methacrylate monomer to a temperature of 25 °C and heating the EGDA monomer to a temperature of 30 °C, to achieve flow rates of 0.6 and 0.9 sccm, respectively. Each polymer film was grown to a 1 μm thickness as measured on a reference silicon wafer using an in situ 633 nm helium–neon laser interferometer (Industrial Fiber Optics). Polymer canopies were imaged using a SEM (Topcon Aquila) and a stereo microscope (National). SEM micrographs were acquired using a 15 kV accelerating voltage on samples that were sputter coated with platinum to prevent charging. EDS was

performed using a SEM (JEOL JSM-7001F) with an EDS detector (EDAX Apollo X).

The [emim][BF₄] used in the Droplet Method was evacuated for 24 h in a desiccator to remove residual water prior to dispensing it onto PDMS micropillar surfaces using a micropipette. After depositing the polymer coating, the polymer film residing on top of the [emim][BF₄] droplet was removed using a pair of tweezers to peel the film off the liquid. The [emim][BF₄] droplet was then removed by submerging the pillars in a methanol bath for 15 min and allowing the solvent to evaporate for 2 h before imaging.

The silicone oil heights used in the Inverted Method were obtained by spin coating 1 mL of silicone oil (1000 cSt) onto a 3.5 × 3.5 cm² wafer using speeds of 4000, 3000, and 2500 rpm with an acceleration of 100 rpm/s for 30 s to obtain thicknesses that produced canopies with heights of 58, 50, and 46 μm, respectively. After spin coating, all silicone oil layers were allowed to rest on a hot plate set at a constant temperature of 60 °C for 60 min to increase film uniformity. PDMS pillars coated with PPFDA were then gently inverted onto the silicone oil layers using a pair of tweezers and covered with a glass slide to prevent the pillars from floating. The inverted samples were then placed under vacuum using the iCVD reactor chamber where the silicone oil was once again heated to 60 °C for an hour to reduce any nonuniform wetting that may have occurred during the inversion of the pillars onto the silicon oil. Afterward, the samples were cooled to the appropriate reactor stage temperature for 20 min before depositing a polymer coating. After the coating was applied, the PDMS substrates were carefully removed from the silicone oil with a pair of tweezers and submerged in hexane for 15 min to wash away any residual silicone oil.

Spreading coefficients were calculated using a goniometer (Ramé-Hart Model 290-F1) to measure advancing contact angles, equilibrium contact angles, liquid–vapor surface tensions, and polymer–vapor surface tensions. Advancing contact angles were measured using the tilting base method. Liquid–vapor surface tensions were measured using the pendant drop method, while polymer–vapor surface tensions were calculated using the acid–base method with equilibrium contact angles from water, glycerol, and diiodomethane. All measurements were performed five times.

AUTHOR INFORMATION

Corresponding Author

*E-mail: malanchg@usc.edu (M.G.).

Notes

The authors declare no competing financial interest.

ACKNOWLEDGMENTS

This work was supported by the National Science Foundation Division of Civil, Mechanical, and Manufacturing Innovation Award Number 1069328.

REFERENCES

- (1) Fuchs, A. D.; Tiller, J. C. Contact-Active Antimicrobial Coatings Derived from Aqueous Suspensions. *Angew. Chem., Int. Ed.* **2006**, *45*, 6759–6762.
- (2) Wu, Z.; Tong, W.; Jiang, W.; Liu, X.; Wang, Y.; Chen, H. Poly(*N*-vinylpyrrolidone)-Modified Poly(dimethylsiloxane) Elastomers As Anti-Biofouling Materials. *Colloids Surf., B* **2012**, *96*, 37–43.
- (3) Schmidt, S.; Motschmann, H.; Hellweg, T.; von Klitzing, R. Thermoresponsive Surfaces by Spin-Coating of PNPAM-*co*-PAA Microgels: A Combined AFM and Ellipsometry Study. *Polymer* **2008**, *49*, 749–756.
- (4) Ma, M.; Gupta, M.; Li, Z.; Zhai, L.; Gleason, K. K.; Cohen, R. E.; Rubner, M. F.; Rutledge, G. C. Decorated Electrospun Fibers Exhibiting Superhydrophobicity. *Adv. Mater.* **2007**, *19*, 255–259.
- (5) Subramani, C.; Ofir, Y.; Patra, D.; Jordan, B. J.; Moran, I. W.; Park, M. H.; Carter, K. R.; Rotello, V. M. Nanoimprinted Polyethyleneimine: A Multimodal Template for Nanoparticle

Assembly and Immobilization. *Adv. Funct. Mater.* **2009**, *19*, 2937–2942.

(6) Chang, J.-P.; El Rassi, Z.; Horváth, C. Silica-Bound Poly-ethyleneglycol As Stationary Phase for Separation of Proteins By High-Performance Liquid Chromatography. *J. Chromatogr.* **1985**, *319*, 396–399.

(7) Gao, Q.; Wu, D.; Sun, Y.; Li, X. pH-Responsive Drug Release from Polymer-Coated Mesoporous Silica Spheres. *J. Phys. Chem. C* **2009**, *113*, 12753–12758.

(8) Tenhaeff, W. E.; Gleason, K. K. Initiated and Oxidative Chemical Vapor Deposition of Polymeric Thin Films: iCVD and oCVD. *Adv. Funct. Mater.* **2008**, *18*, 979–992.

(9) Susut, C.; Timmons, R. B. Plasma Enhanced Chemical Vapor Depositions to Encapsulate Crystals in Thin Polymeric Films: a New Approach to Controlling Drug Release Rates. *Int. J. Pharm.* **2005**, *288*, 253–261.

(10) Baxamusa, S. H.; Im, S. G.; Gleason, K. K. Initiated and Oxidative Chemical Vapor Deposition: a Scalable Method for Conformal and Functional Polymer Films on Real Substrates. *Phys. Chem. Chem. Phys.* **2009**, *11*, 5227–5240.

(11) Bose, R. K.; Nejadi, S.; Stuffle, D. R.; Lau, K. K. S. Graft Polymerization of Anti-Fouling PEO Surfaces by Liquid-Free Initiated Chemical Vapor Deposition. *Macromolecules* **2012**, *45*, 6915–6922.

(12) Kwong, P.; Gupta, M. Vapor Phase Deposition of Functional Polymers onto Paper-Based Microfluidic Devices for Advanced Unit Operations. *Anal. Chem.* **2012**, *84*, 10129–10135.

(13) Chen, B.; Kwong, P.; Gupta, M. Patterned Fluoropolymer Barriers for Containment of Organic Solvents within Paper-Based Microfluidic Devices. *ACS Appl. Mater. Interfaces* **2013**, *5*, 12701–12707.

(14) Kwong, P.; Seidel, S.; Gupta, M. Effect of Transition Metal Salts on the Initiated Chemical Vapor Deposition of Polymer Thin Films. *J. Vac. Sci. Technol. A* **2015**, *33*, 031504.

(15) Chen, B.; Seidel, S.; Hori, H.; Gupta, M. Self-Assembly of Pillars Modified with Vapor Deposited Polymer Coatings. *ACS Appl. Mater. Interfaces* **2011**, *3*, 4201–4205.

(16) Lau, K. K. S.; Bico, J.; Teo, K. K. B. K.; Chhowalla, M.; Amaratunga, G. A. J.; Milne, W. I.; McKinley, G. H.; Gleason, K. K. Superhydrophobic Carbon Nanotube Forests. *Nano Lett.* **2003**, *3* (12), 1701–1705.

(17) Frank-Finney, R. J.; Haller, P. D.; Gupta, M. Ultrathin Free-Standing Films Deposited onto Patterned Ionic Liquids and Silicone Oil. *Macromolecules* **2012**, *45*, 165–170.

(18) Frank-Finney, R. J.; Bradley, L. C.; Gupta, M. Formation of Polymer-Ionic Liquid Gels Using Vapor Phase Precursors. *Macromolecules* **2013**, *46*, 6852–6857.

(19) Haller, P. D.; Gupta, M. Synthesis of Polymer Nanoparticles via Vapor Phase Deposition onto Liquid Substrates. *Macromol. Rapid Commun.* **2014**, *35*, 2000–2004.

(20) Bradley, L. C.; Gupta, M. Copolymerization of 1-Ethyl-3-Vinylimidazolium Bis(trifluoromethylsulfonyl)imide via Initiated Chemical Vapor Deposition. *Macromolecules* **2014**, *47*, 6657–6663.

(21) Bradley, L. C.; Gupta, M. Microstructured Films Formed on Liquid Substrates via Initiated Chemical Vapor Deposition of Cross-Linked Polymers. *Langmuir* **2015**, *31*, 7999–8005.

(22) Berg, M. C.; Zhai, L.; Cohen, R. E.; Rubner, M. F. Controlled Drug Release from Porous Polyelectrolyte Multilayers. *Biomacromolecules* **2006**, *7*, 357–364.

(23) Wu, J.; Sailor, M. J. Chitosan Hydrogel-Capped Porous SiO₂ as a pH Responsive Nano-Valve for Triggered Release of Insulin. *Adv. Funct. Mater.* **2009**, *19*, 733–741.

(24) Zhang, Y.; Ang, C. Y.; Li, M.; Tan, S. Y.; Qu, Q.; Luo, Z.; Zhao, Y. Polymer-Coated Hollow Mesoporous Silica Nanoparticles for Triple-Responsive Drug Delivery. *ACS Appl. Mater. Interfaces* **2015**, *7*, 18179–18187.

(25) Ismagilov, R. F.; Ng, J. M. K.; Kenis, P. J. A.; Whitesides, G. M. Microfluidic Arrays of Fluid-Fluid Diffusional Contacts as Detection Elements and Combinatorial Tools. *Anal. Chem.* **2001**, *73*, 5207–5213.

(26) Krumpfer, J. W.; Bian, P.; Zheng, P.; Gao, L.; McCarthy, T. J. Contact Angle Hysteresis on Superhydrophobic Surfaces: An Ionic Liquid Probe Fluid Offers Mechanistic Insight. *Langmuir* **2011**, *27*, 2166–2169.

(27) Seiwert, J.; Clanet, C.; Quéré, D. Coating of a Textured Solid. *J. Fluid Mech.* **2011**, *669*, 55–63.

(28) Smith, J. D.; Dhiman, R.; Anand, S.; Reza-Garduno, E.; Cohen, R. E.; McKinley, G. H.; Varanasi, K. K. Droplet Mobility on Lubricant-Impregnated Surface. *Soft Matter* **2013**, *9*, 1772–1780.

(29) Princen, H. M. Capillary Phenomena in Assemblies of Parallel Cylinders: I. Capillary Rise between Two Cylinders. *J. Colloid Interface Sci.* **1969**, *30*, 69–75.

(30) Princen, H. M. Capillary Phenomena in Assemblies of Parallel Cylinders: II. Capillary Rise in Systems with More than Two Cylinders. *J. Colloid Interface Sci.* **1969**, *30*, 359–371.

(31) Haller, P. D.; Frank-Finney, R. J.; Gupta, M. Vapor-Phase Free Radical Polymerization in the Presence of an Ionic Liquid. *Macromolecules* **2011**, *44* (8), 2653–2659.

(32) Haller, P. D.; Bradley, L. C.; Gupta, M. Effect of Surface Tension, Viscosity, and Process Conditions on Polymer Morphology Deposited at the Liquid-Vapor Interface. *Langmuir* **2013**, *29*, 11640–11645.

(33) Extrand, C. W. Criteria for Ultralyophobic Surfaces. *Langmuir* **2004**, *20*, 5013–5018.

(34) Patankar, N. A. Transition between Superhydrophobic States on Rough Surfaces. *Langmuir* **2004**, *20*, 7097–7102.

(35) Lee, J. B.; Gwon, H. R.; Lee, S. H.; Cho, M. Wetting Transition Characteristics on Microstructured Hydrophobic Surfaces. *Mater. Trans.* **2010**, *51*, 1709–1711.

(36) Bhushan, B.; Nosonovsky, M.; Jung, Y. C. Towards Optimization of Patterned Superhydrophobic Surfaces. *J. R. Soc., Interface* **2007**, *4*, 643–648.

(37) Yang, S.; Khare, K.; Lin, P. C. Harnessing Surface Wrinkle Patterns in Soft Matter. *Adv. Funct. Mater.* **2010**, *20*, 2550–2564.

(38) Bradley, L. C.; Gupta, M. Formation of Heterogeneous Polymer Films via Simultaneous or Sequential Depositions of Soluble and Insoluble Monomers onto Ionic Liquids. *Langmuir* **2013**, *29*, 10448–10454.

(39) Riche, C. T.; Marin, B. C.; Malmstadt, N.; Gupta, M. Vapor Deposition of Cross-linked Fluoropolymer Barrier Coatings onto Pre-Assembled Microfluidic Devices. *Lab Chip* **2011**, *11*, 3049–3052.

(40) Chen, B.; Riche, C. T.; Lehmann, M.; Gupta, M. Responsive Polymer Welds via Solution Casting for Stabilized Self-Assembly. *ACS Appl. Mater. Interfaces* **2012**, *4*, 6911–6916.